

Atomic-Weight Dependence of the Production of Hadron Pairs by 800-GeV/c Protons on Nuclear Targets

K. Streets,^(a) G. Boca,^(b) C. Georgiopoulos, J. H. Goldman, S. Hagopian, V. Hagopian, K. F. Johnson, D. M. Kaplan,^(c) D. Levinthal, F. Lopez,^(d) H. L. Sawyer, J. Streets,^(e) H. B. White,^(f) and C. Young
Florida State University, Tallahassee, Florida 32306

M. Crisler, A. Lathrop, and S. Pordes
Fermi National Accelerator Laboratory, Batavia, Illinois 60510

J. Volk^(e)
University of California at Davis, Davis, California 95616

M. Cummings and H. R. Gustafson
University of Michigan, Ann Arbor, Michigan 48109
 (Received 8 November 1990)

Fermilab experiment 711 has investigated proton-nucleus collisions in which two high-transverse-momentum hadrons are produced forming high-mass ++, +-, and -- charged states, using an 800-GeV/c proton beam on targets of beryllium, aluminum, iron, and tungsten. Our data cover the range in dihadron mass from 6 to 15 GeV/c². We show here that the dependence of the cross section on atomic weight A can be parametrized as A^α , where $\alpha = 1.043 \pm 0.011(\text{stat}) \pm 0.025(\text{syst})$, and is independent of the charge state of the dihadron system.

PACS numbers: 13.85.Ni, 12.38.Qk, 25.40.Ve

Since its discovery in 1972,¹ high-transverse-momentum hadronic production has been used to study QCD.² The interpretation of data on the production of a single high- p_t particle is complicated, however, by effects due to the intrinsic motion of the partons. Data from nuclear targets³ may be further complicated both by collective nuclear effects on the intrinsic motion of the partons⁴ and by interactions of the scattered partons with the nuclear matter. Experiments analyzing dijet production from nuclei have observed large nuclear effects depending on the kinematics of the jet; when the cross sections are parametrized in the form $\sigma(A) = \sigma_0 A^\alpha$, values of α between 1.14 and 1.48 have been measured.⁵ A technique⁶ which avoids these effects is to select events in which two individual high-transverse-momentum hadrons are produced, roughly back to back, to form a high-mass state. By requiring two back-to-back particles, the sensitivity to the intrinsic transverse parton momentum is minimized. Data from leptonic interactions,⁷ moreover, show that nuclear effects are small (negligible for our purposes) in leading-particle production. The present experiment was designed to test the hard-scattering predictions of QCD in hadronic collisions by observing high-mass dihadron events produced in proton-nucleus collisions. We present data on the dependence of the cross section with atomic weight (A) for the production of pairs of charged hadrons on four nuclear targets; the data cover the mass range between 6 and 15 GeV/c² and are presented for ++, +-, and -- charged states.

The detector⁸ (Fig. 1) consisted of a high-resolution magnetic spectrometer with a calorimeter trigger and was designed to have a large acceptance for all charge states in both the polar angle defined in the rest frame of the massive state ($|\cos\theta^*| < 0.5$) and in the central rapidity region in the proton-nucleon center of mass ($|Y_{pN}| < 0.5$). A 1-mm-wide, 10%-interaction-length target was placed just upstream of two large-aperture analysis magnets, which provided a momentum kick of 1.16 GeV/c in the horizontal plane. Downstream of the magnets were five wire chambers (four views per chamber) to reconstruct charged-particle tracks, four planes of scintillation hodoscopes to identify charged particles, and two calorimeters to provide the trigger. To allow the experiment to operate at high rates [(2-5) × 10⁶ interactions/s], the apparatus was made insensitive in the median plane and covered the region from 20 to 100 mrad in the vertical direction. The calorimeters were

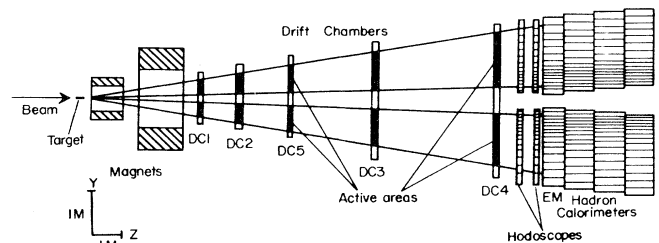


FIG. 1. E711 detector, nonbend view.

TABLE I. Luminosity for each target. L_n is the luminosity for nuclei. L_N is the luminosity for nucleons, and is $L_n A$.

Material	L_n (nb ⁻¹)	L_N (pb ⁻¹)
Beryllium	1774	15.98
Aluminum	225.8	6.090
Iron	275.6	15.39
Tungsten	35.34	6.497

each comprised of 16 horizontal segments and covered the azimuthal region from 65° to 115° and 245° to 295°.

The trigger required a total transverse energy in the calorimeters of greater than 6 GeV with a localized transverse-energy deposition in each calorimeter of greater than 2 GeV. Charged hadrons were selected by requiring signals from the corresponding hodoscope elements in front of the energy clusters. Triggering on particles that scatter in the vertical plane and measuring momenta by bending in the horizontal plane minimized the effect of the magnetic bending on the trigger. This allowed the use of a high magnetic field and a long lever arm, thus improving the momentum resolution. The target defined the interaction vertex, eliminating the need for track measurements upstream of the magnets.

The determination of α relies on the measurement of the relative luminosity and number of events produced for each nuclear target. To set a scale, an error of 10%

in the relative cross sections for Be and W corresponds to an error in α of 3.3%. Since data were taken in periods of 2-3 weeks on each target, care was taken to monitor and correct for changes in luminosity calibration, trigger efficiency, and event-reconstruction efficiency over the course of the run.

The amount of beam hitting the target, typically 90% of the total beam, was measured continuously by four independent sets of triple-coincidence scintillation-counter telescopes placed symmetrically around the target and at 90° to the beam. This system was calibrated several times for each target by sweeping the beam horizontally across the target, while monitoring the total beam flux with an ion chamber upstream of the experiment. The luminosity distributions from the four telescopes showed a Gaussian beam profile convoluted with the target profile, and a flat background ($\approx 10\%$) proportional to the total beam flux. This background rate remained constant throughout the data taking (within 3% of itself) and was equal to the rate with the target material removed. The ion chamber was calibrated periodically with scintillation counters at low beam intensity and found to be stable within $\pm 2\%$. The integrated luminosities as given by the four telescopes agreed to within 3% for each target. We have assigned an overall systematic uncertainty of 4% in the value of the luminosity. Statistical errors are negligible. The integrated luminosities for each target type are listed in Table I.

Particle momenta⁹ were calculated from the down-

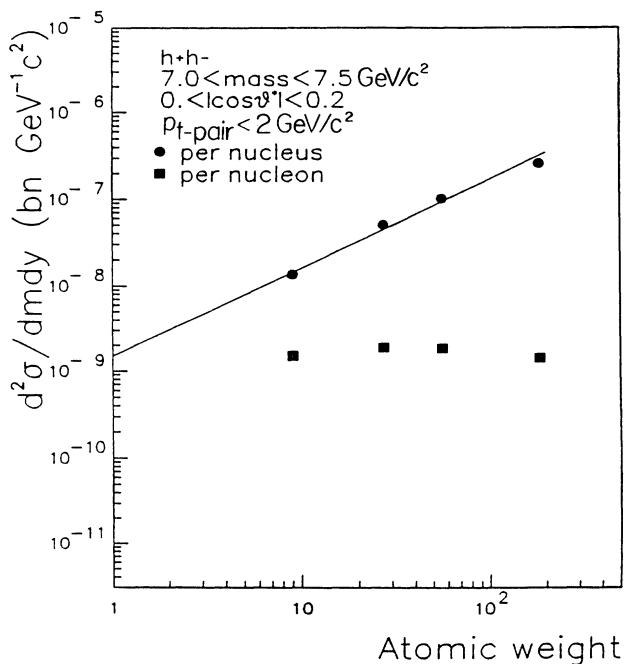


FIG. 2. Differential cross section vs atomic weight for the four targets. The line is a fit by the form $\ln(d^2\sigma/dM dY) = \alpha \ln A + \ln C$.

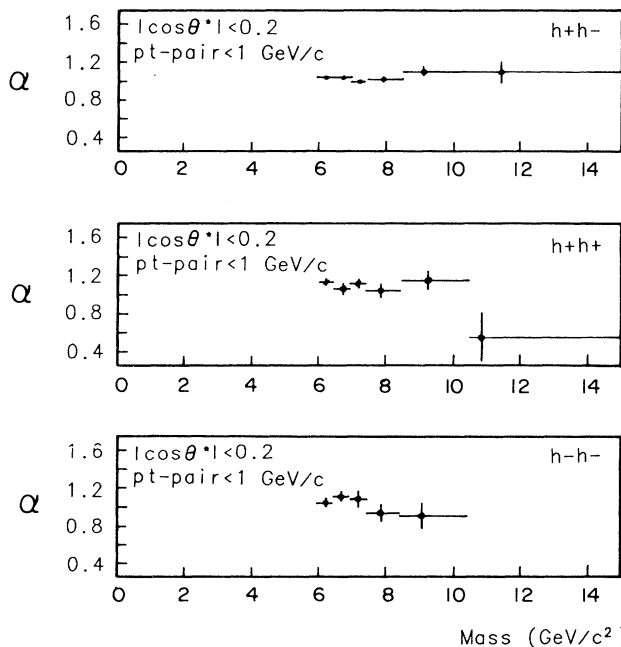


FIG. 3. α vs mass of hadron pair for $p_{t,pair} < 1.0$ GeV/c for +-, ++, and -- charged states.

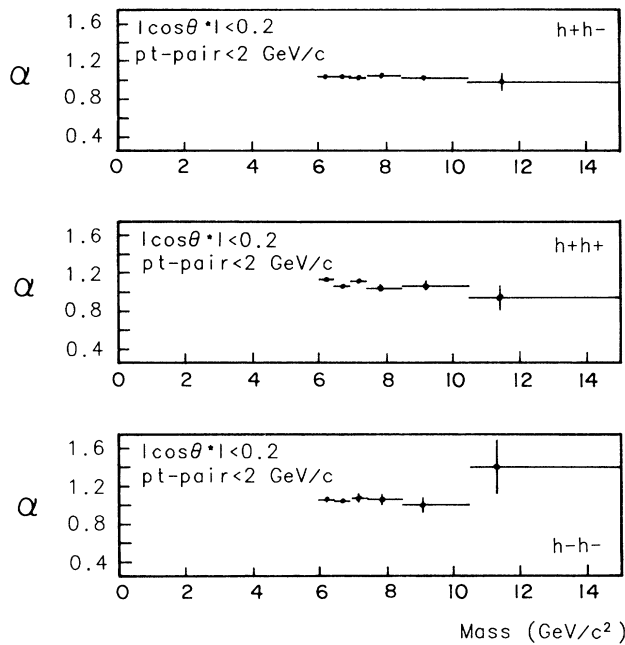


FIG. 4. α vs mass of hadron pair for $p_{t, \text{pair}} < 2.0 \text{ GeV}/c$ for $+-$, $++$, and $--$ charged states.

stream trajectory, assuming that the interaction occurred at the center of the target. The reconstruction efficiency for data from each target was calculated separately. The efficiency for a single track was determined by inserting fake tracks, generated with observed chamber efficiencies, into the data and measuring the reconstruction rate. This efficiency was measured to vary between 76% and 89% for single tracks, due to changes in chamber operating conditions. The systematic uncertainty in the event-reconstruction efficiency is estimated to be 8%, which corresponds to the largest change between consecutive measurements. The momentum resolution $\delta p/p$ was better than $3 \times 10^{-4} p$ (p in GeV/c) and corrections to the mass spectrum due to this resolution are negligible. To ensure complete shower containment in the calorimeter, the range of rapidity and center-of-mass polar angle was restricted to be $-0.4 < Y_{pN} < 0.2$ and $|\cos \theta^*|$

< 0.2 . The acceptance in this region was between 0.1 and 0.2, and variations within any mass bin were negligible.

The trigger threshold was measured continuously by using data accumulated with a prescaled trigger at a lower-mass threshold. The trigger efficiency was $60\% \pm 3\%$ at $6 \text{ GeV}/c^2$, the lowest mass used here for analysis, and 100% above $7.5 \text{ GeV}/c^2$.

The high-mass dihadrons were selected by requiring that the tracks projected back to the target in the non-bend view were within $\pm 5\sigma$ of the center of the target, that the dihadron alone satisfied the trigger, and that the track momenta matched the associated calorimeter energies within 5σ . The most significant background was from proton interactions in material other than the target (mainly air). Several target-out runs were taken and the data were analyzed in the same manner as the normal data. The target-out data had a similar spectrum to the target-in data and resulted in background subtractions to the final data samples of 2.7% for Be, 1.4% for Al, 1.2% for Fe, and 1.0% for W. Given the interaction rate, accidental triggers from the overlap of two independent events are negligible.

The dependence of the event yield per unit luminosity on atomic weight has been parametrized in the form $\ln \sigma(A) = \alpha \ln A + \ln \sigma_0$. The data have been fitted as a function of the dihadron mass M_{pair} and the charge state of the pair for two ranges of the net transverse momentum $p_{t, \text{pair}}$. Figure 2 shows the cross section per nucleus and per nucleon versus atomic weight for each of the four targets in the mass range $7 < M_{\text{pair}} < 7.5 \text{ GeV}/c^2$ and for the $+-$ charge state. The results of the fits for α are shown as a function of mass for the three different charge states in Fig. 3 ($p_{t, \text{pair}} < 1 \text{ GeV}/c$) and Fig. 4 ($p_{t, \text{pair}} < 2 \text{ GeV}/c$). The numerical values with their statistical errors are presented in Tables II and III. The average values of α over the full mass range for the three charge states for $p_{t, \text{pair}} < 1$ and $< 2 \text{ GeV}/c$ are 1.042 ± 0.011 and 1.049 ± 0.007 , respectively. The total systematic error of 12% is due to the uncertainty in the track reconstruction and luminosity measurement and corresponds to an average systematic error in α of 0.025.

The fit by the form $\sigma(A) = \sigma_0 A^\alpha$ shows that α is close

TABLE II. Atomic-weight dependence (α) for $P_T \leq 1 \text{ GeV}/c$.

Mass range (GeV/c^2)	Charge state		
	$+-$	$++$	$--$
6.0-6.5	1.034 ± 0.019	1.130 ± 0.040	1.043 ± 0.049
6.5-7.0	1.033 ± 0.024	1.054 ± 0.051	1.111 ± 0.064
7.0-7.5	0.988 ± 0.035	1.117 ± 0.061	1.079 ± 0.086
7.5-8.5	1.015 ± 0.037	1.041 ± 0.072	0.944 ± 0.102
8.5-10.5	1.101 ± 0.059	1.130 ± 0.102	0.916 ± 0.147
10.5-15.0	1.091 ± 0.127	0.553 ± 0.256	
6.0-15.0	1.029 ± 0.012	1.093 ± 0.025	1.049 ± 0.033

TABLE III. Atomic-weight dependence (α) for $P_T \leq 2 \text{ GeV}/c$.

Mass range (GeV/c^2)	Charge state		
	$+-$	$++$	$--$
6.0-6.5	1.035 ± 0.012	1.125 ± 0.022	1.060 ± 0.029
6.5-7.0	1.042 ± 0.016	1.052 ± 0.028	1.051 ± 0.041
7.0-7.5	1.030 ± 0.022	1.102 ± 0.036	1.069 ± 0.053
7.5-8.5	1.045 ± 0.023	1.026 ± 0.042	1.059 ± 0.056
8.5-10.5	1.025 ± 0.037	1.046 ± 0.059	0.992 ± 0.093
10.5-15.0	0.976 ± 0.093	0.932 ± 0.126	1.407 ± 0.274
6.0-15.0	1.036 ± 0.008	1.085 ± 0.014	1.058 ± 0.020

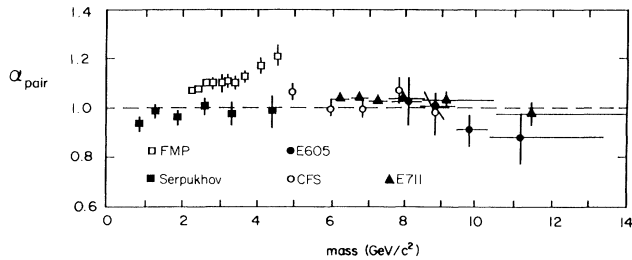


FIG. 5. α vs mass for the $+-$ charge state for experiments measuring hadron pair production.

to unity for both $p_{t,\text{pair}} < 1$ and < 2 GeV/c for the $++$, $+-$, and $--$ charge states. We observe no significant variation over our mass range. This is in agreement with most published results for unlike-sign dihadrons¹⁰ (see Fig. 5). There are no previously published data on like-sign hadron pairs. These results are consistent with the calculations of Lev and Petersson;¹¹ however, the increase of α with $p_{t,\text{pair}}$ predicted by this model would be too small to be seen with these data.

The National Science Foundation and the U.S. Department of Energy funded this work. We thank the staffs of Fermilab and Florida State University for their technical support.

^(a)Now at University of Maryland, College Park, MD 20742.

^(b)Now at University of Pavia, Pavia, Italy.

^(c)Now at Northern Illinois University, DeKalb, IL 60115.

^(d)Now at Argonne National Laboratory, Argonne, IL 60439.

^(e)Now at Fermi National Accelerator Laboratory, Batavia, IL 60510.

^(f)On leave from Fermi National Accelerator Laboratory, Batavia, IL 60510.

¹B. Alper *et al.*, Phys. Lett. **44B**, 521 (1973); F. W. Busser *et al.*, Phys. Lett. **46B**, 471 (1973).

²S. Berman, J. Bjorken, and J. Kogut, Phys. Rev. D **4**, 3388 (1971); B. L. Combridge, J. Kripfganz, and J. Ranft, Phys. Lett. **70B**, 234 (1977).

³D. Antreasyan *et al.*, Phys. Rev. D **19**, 764 (1979), and references therein.

⁴A. Bodek and J. L. Ritchie, Phys. Rev. D **23**, 1070 (1981); **24**, 1400 (1981).

⁵H. E. Miettinen, Phys. Lett. B **207**, 222 (1988).

⁶J. Owens, Phys. Rev. D **20**, 221 (1979); R. Baier, J. Engels, and B. Petersson, Z. Phys. C **2**, 265 (1979); J. Gunion and B. Petersson, Phys. Rev. D **22**, 629 (1980).

⁷A. Arvidson *et al.*, Nucl. Phys. **B246**, 381 (1984).

⁸K. Streets, Ph.D. dissertation, Florida State University, 1989 (unpublished).

⁹C. H. Georgiopoulos, J. H. Goldman, and M. Hodous, Nucl. Instrum. Methods Phys. Res., Sect. A **261**, 493 (1987).

¹⁰R. L. McCarthy *et al.*, Phys. Rev. Lett. **40**, 213 (1978); D. A. Finley *et al.*, Phys. Rev. Lett. **42**, 1031 (1979); V. V. Abramov *et al.*, Pis'ma Zh. Eksp. Teor. Fiz. **38**, 296 (1983) [JETP Lett. **38**, 352 (1983)]; Y. B. Hsiung *et al.*, Phys. Rev. Lett. **55**, 457 (1985).

¹¹M. Lev and B. Petersson, Z. Phys. C **21**, 155 (1983).